

# BeppoSAX serendipitous discovery of the X-ray pulsar SAX J1802.7–2017

G. Augello<sup>1</sup>, R. Iaria<sup>1</sup>, N. R. Robba<sup>1</sup>, T. Di Salvo<sup>1,2</sup>, L. Burderi<sup>3</sup>, G. Lavagetto<sup>1</sup>, L. Stella<sup>3</sup>

## ABSTRACT

We report on the serendipitous discovery of a new X-ray source, SAX J1802.7–2017,  $\sim 22'$  away from the bright X-ray source GX 9+1, during a BeppoSAX observation of the latter source on 2001 September 16–20. SAX J1802.7–2017 remained undetected in the first 50 ks of observation; the source count rate in the following  $\sim 300$  ks ranged between 0.04 c/s and 0.28 c/s, corresponding to an averaged 0.1–10 keV flux of  $3.6 \times 10^{-11}$  ergs cm $^{-2}$  s $^{-1}$ . We performed a timing analysis and found that SAX J1802.7–2017 has a pulse period of 139.612 s, a projected semimajor axis of  $a_x \sin i \sim 70$  lt-s, an orbital period of  $\sim 4.6$  days and a mass function  $f(M) \sim 17 \pm 5 M_{\odot}$ . The new source is thus an accreting X-ray pulsar in a (possibly eclipsing) high mass X-ray binary. The source was not detected by previous X-ray astronomy satellites, indicating that it is likely a transient system.

*Subject headings:* stars: neutron — stars: magnetic fields — pulsars: general — pulsars: individual: SAX J1802.7–2017 — X-ray: binaries

## 1. Introduction

High mass X-ray binaries (hereafter HMXBs) are young systems, and the neutron stars (NSs) that are often hosted in them usually have a strong magnetic field ( $B \sim 10^{12}$  Gauss). Accretion onto these NSs occurs via capture of stellar wind matter and Roche-lobe overflow. HMXBs comprise two main subgroups: a) the supergiant systems, and b) the Be star systems.

---

<sup>1</sup>Dipartimento di Scienze Fisiche ed Astronomiche, Università di Palermo, via Archirafi 36 - 90123 Palermo, Italy; email: augello@gifco.fisica.unipa.it, iaria@gifco.fisica.unipa.it, robba@gifco.fisica.unipa.it

<sup>2</sup>Astronomical Institute "Anton Pannekoek," University of Amsterdam and Center for High-Energy Astrophysics, Kruislaan 403, NL 1098 SJ Amsterdam, the Netherlands; email: disalvo@science.uva.nl

<sup>3</sup>Osservatorio Astronomico di Roma, via Frascati 33, 00040 Monteporzio Catone (Roma), Italy; email: burderi@mporzio.astro.it, stella@mporzio.astro.it

In the supergiant systems, the companion is of spectral type earlier than B2 and has evolved off the main sequence. Orbital periods are generally less than 10 days, orbits are circular, and the mass transfer takes place because of the strong stellar wind from the OB star and/or because of “incipient” Roche Lobe overflow. The Be star systems are characterized by emission lines (mainly the Balmer series) which originate in the equatorial circumstellar envelope of the companion star. The orbital periods in these systems tend to be longer than those of group a) and correlate well with the pulsar spin period (Corbet 1986). The orbits are usually moderately eccentric. Transient activity is common in Be HMXBs; different types of outburst have been observed from different sources, and occasionally also from the same source. Giant outbursts involve high peak luminosities, occur at any orbital phase and show only little (if any) orbital modulation of the X-ray flux. Recurrent outbursts usually involve lower peak luminosities, tend to occur close to periastron and sometimes show a strong modulation of the X-ray flux with the orbital phase (see e.g. Stella, White, & Rosner 1986). To date, about 80 HMXBs are known;  $\sim 40$  of them show periodic X-ray pulsations with spin periods distributed over a wide range from 69 ms to  $\sim 24$  min (see Nagase 1989 for a review).

While studying the atoll source GX 9+1 with BeppoSAX, we have discovered a new X-ray pulsator in a HMXB. We report here the results of the timing analysis of this new X-ray source.

## 2. Observations

The observation of the GX 9+1 field was carried out from 2001 September 16 02:01:30.0 (UTC) to 2001 September 20 03:00:08.5 (UTC), using the co-aligned Narrow Field Instruments (NFIs) on board BeppoSAX. These are: a Low Energy Concentrator Spectrometer (LECS; energy range 0.1–10 keV; Parmar et al. 1997), two Medium Energy Concentrator Spectrometers (MECS; energy range 1–10 keV; Boella et al. 1997), a High Pressure Gas Scintillation Proportional Counter (HPGSPC; energy range 7–60 keV; Manzo et al. 1997), and a Phoswich Detector System (PDS; energy range 13–200 keV; Frontera et al. 1997). The exposure times were  $\sim 60$  ks,  $\sim 149$  ks,  $\sim 142$  ks,  $\sim 71$  ks, for LECS, MECS, HPGSPC and PDS, respectively. The circular field of view (FOV) of the LECS and MECS is  $37'$  and  $56'$  in diameter, respectively, while those of the HPGSPC and PDS are hexagonal with FWHM of  $78'$  and  $66'$ , respectively. The LECS and MECS detectors are position sensitive counters with imaging capability. The position reconstruction uncertainty for MECS is  $0.5'$  in the central area of  $9'$  radius, and  $\sim 1.5'$  in the outer region of the FOV (Boella et al. 1997). The HPGSPC and PDS systems do not have imaging capabilities, and their data are therefore

difficult to interpret and analyse for individual sources when the FOV includes more than one source.

Figure 1 shows the BeppoSAX/MECS image (1-10 keV) centered at the position of the bright atoll source GX 9+1. A fainter source is visible at R.A.(2000.0)= 18h 02m 39.9s and Dec.(2000.0)=  $-20^\circ 17' 13.50''$  (position uncertainty  $2'$ ), at an angular distance from GX 9+1 of  $\sim 22'$ . The source was outside the FOV of the BeppoSAX/LECS. We have verified its presence in both the MECS2 and MECS3 images, which probably excludes that this was a ghost image of a source outside the MECS FOV. Moreover, we can be sure that the source was within the PDS FOV, because the source X-ray pulsations were also detected in the PDS data (see below). We searched for known X-ray sources in a circular region of  $30'$  centered at GX 9+1 in the SIMBAD data base. We found no known sources with a position compatible with that of the faint source; we therefore designate this serendipitous source as SAX J1802.7–2017.

We extracted the MECS events of SAX J1802.7–2017 from an elliptical region centered at R.A.(2000.0)= 18h 02m 39.9s and Dec.(2000.0)=  $-20^\circ 17' 13.50''$  and the background events from an elliptical region similar to the one used for the source, centered at a symmetric position with respect to the center of the MECS FOV and not contaminated by GX 9+1 (see Fig. 1). In Figure 2 the lightcurves of SAX J1802.7–2017 plus background (crosses) and of the background (stars) are shown. The source was not detected during the first 50 ks when the count rate within the extraction region ( $0.034 \pm 0.001$  c/s) was compatible with the background count rate. In the following  $\sim 300$  ks the source count rate showed a large variability with an average intensity significantly above the background level. Two flaring events took place  $\sim 110$  ks and  $\sim 300$  ks from the beginning of the observation.

### 3. Temporal Analysis

The arrival time of all events in the MECS and PDS were corrected to the solar system barycenter. We searched for periodicities by computing a Power Spectrum Density (PSD) in the range between  $4 \times 10^{-4}$  Hz and 1 kHz from Fast Fourier Transforms (FFTs) performed on MECS data of SAX J1802.7–2017.

A main peak at a frequency of  $\sim 7.20$  mHz, corresponding to a period of  $\sim 139$  s, is evident (see Fig. 3). The second harmonic is also clearly visible. We performed a folding search for periods centered around  $\sim 139$  s finding a not well defined period, because two  $\chi^2$  peaks were present at  $\sim 139.49$  s and  $\sim 139.70$  s, respectively.

To study possible delays in the pulse arrival times, or, equivalently, pulse period vari-

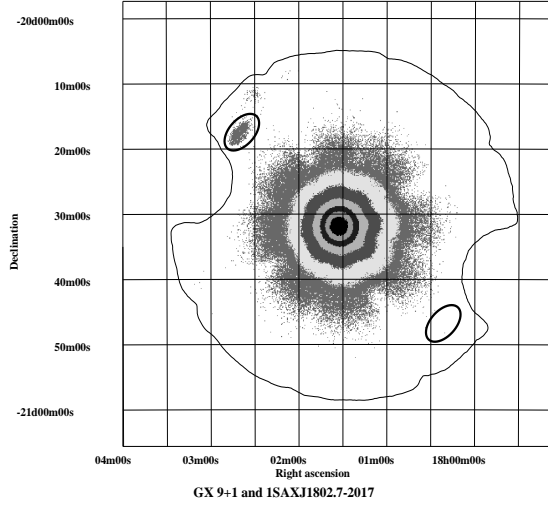


Fig. 1.— BeppoSAX/MECS image (1-10 keV) of the GX 9+1 field. SAX J1802.7–2017 is visible at the top left. Its angular separation from GX 9+1 is  $\sim 22'$ . The extraction region of the source and background are also shown. The two semi-circular “cut-outs” are due to the removal of internal calibration source events.

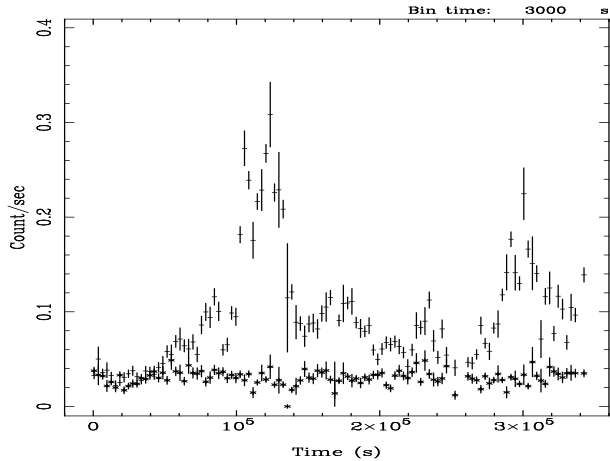


Fig. 2.— MECS Lightcurves (1-10 keV) of SAX J1802.7–2017 plus background (crosses) and of the background (stars). The bin time is 3000 s.

ations we divided the whole data set into 35 consecutive intervals each having a length of about 10 ks. We found that only 27 of these intervals had enough statistics to carry out the analysis described below. A folding search was performed in each interval for a range of trial periods centered around 139 s. The corresponding best periods were obtained by fitting the  $\chi^2$  versus trial period curve with a Gaussian function. The best periods varied significantly and with continuity between 139.44 s and 139.86 s with an average value of 139.608 s.

Phase delays (Fig. 4) were obtained by cross-correlating the folded lightcurves obtained for each of the 27 intervals with that of the whole observation used as a template (an average pulse period of 139.608 s was adopted in the folding). Initially we fitted the phase delays  $\Delta\phi$  using

$$\Delta\phi = a_0 + a_1 t_n + a_2 t_n^2, \quad (1)$$

where  $t_n$  is the arrival time of the  $n$ th pulse. In this formula the linear term  $a_1 = \Delta P_{pulse}/P_{pulse}^2$  and the quadratic term  $a_2 = \dot{P}_{pulse}/2P_{pulse}^2$  are related to a correction to the pulse period and the derivative of the pulse period, respectively. We obtained a  $\chi^2_{red}$  of 2.6 indicating that the modulation of the phase delays cannot only be explained by the presence of a derivative of the pulse period. Moreover we find a value of  $\dot{P}_{pulse}/P_{pulse}$  of  $0.40 \pm 0.01 \text{ yr}^{-1}$ , more than an order of magnitude larger than the largest measured value in any known X-ray pulsar (i.e.  $-10^{-2} \text{ yr}^{-1}$  in GX 1+4, see Pereira et al. 1999). We checked whether the modulation of the phase delays could be explained by the propagation delays due to the orbital motion of the X-ray pulsar around a companion star by fitting the phases with

$$\Delta\phi = a_0 + a_1 t_n + B \cos \left[ \frac{2\pi(t_n - T_{\pi/2})}{P_{orb}} \right], \quad (2)$$

The results of the fit are reported in Table 1. The  $\chi^2_{red}$  was 1.3. Since  $a_x \sin i = P_{pulse}B$ , we find  $a_x \sin i \sim 70 \text{ lt-s}$ ; the corrected pulse period was  $\sim 139.612 \text{ s}$ .

We tried to add a quadratic term to expression (2) to take into account a spin period derivative, but, because of the small number of points and a relatively short observation, we could not constrain all parameters of the fit. In any case, by fixing the quadratic term in the range  $-9 \times 10^{-3} - 9 \times 10^{-3} \text{ days}^{-2}$  (corresponding to a  $\dot{P}_{pulse}/P_{pulse}$  in the range  $-10^{-2} - 10^{-2} \text{ yr}^{-1}$ ) we found that the orbital parameters do not change significantly ( $\sim 2\%$  changes in the orbital period value and  $\sim 4\%$  in the  $a_x \sin i$  value) with respect to the parameters reported in Table 1.

We corrected the arrival times of all the events, observed by the MECS and PDS instruments, to the center of mass of the binary system using the orbital parameters and the corrected pulse period reported in Table 1. We then re-computed, on the corrected folded lightcurves, the phase delays, and found that they are compatible with zero phase delay

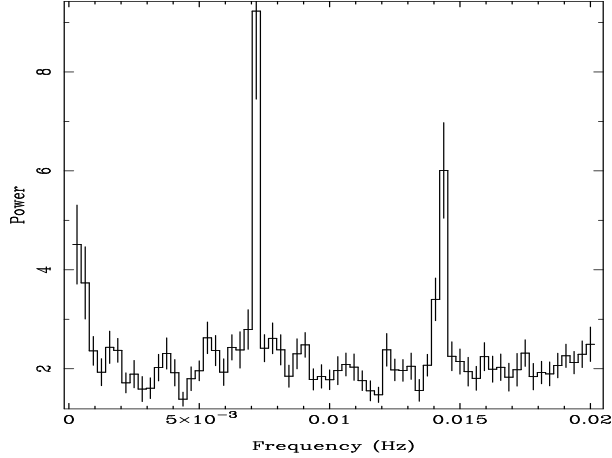


Fig. 3.— Power spectrum density of SAX J1802.7–2017 obtained from MECS data (1.0–10.5 keV energy band) extracted from an elliptical region centered on the source as described in the text. 61 PSDs, computed from time intervals of  $\sim 5$  ks length, were averaged. The fundamental and second harmonic are clearly visible at 7.2 mHz and 14.4 mHz, respectively. The PSD is normalized according to prescription of Leahy et al. (1983).

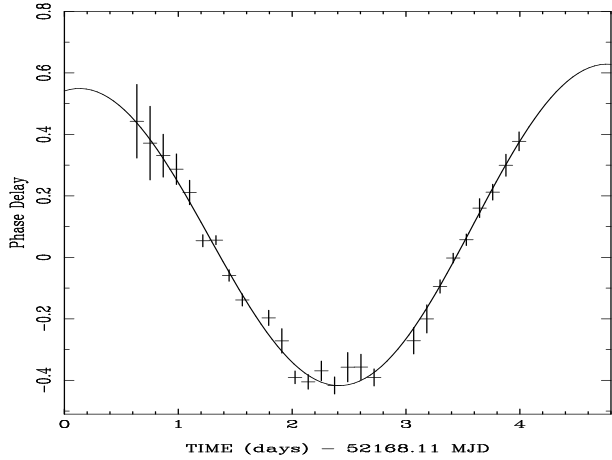


Fig. 4.— Phase delays of SAX J1802.7–2017 as a function of time. The solid line is the best fit function (2) discussed in the text; the orbital period is  $\sim 4.6$  days.

Table 1: Orbital parameters of SAX J1802.7–2017. Errors are at  $1\sigma$  confidence level.

| Parameter    | Value                          |
|--------------|--------------------------------|
| $a_0$        | $0.04^{+0.12}_{-0.09}$         |
| $a_1$        | $0.02 \pm 0.03$ days $^{-1}$   |
| $B$          | $0.50^{+0.07}_{-0.05}$         |
| $P_{orb}$    | $4.6^{+0.4}_{-0.3}$ days       |
| $a_x \sin i$ | $70^{+10}_{-7}$ lt-s           |
| $T_{\pi/2}$  | $52168.22^{+0.10}_{-0.12}$ MJD |
| $P_{pulse}$  | $139.612^{+0.006}_{-0.007}$ s  |

(see Fig. 5). This suggests that our data are compatible with a circular orbit, although an eccentricity could be present but not appreciated because of the relatively low statistics of our data. To estimate a rough upper limit to the eccentricity of the system, we fitted our phase delays substituting the circular orbital correction in equation (2) with a first-order approximation of the eccentric orbital correction (see e.g. van der Klis & Bonnet-Bidaud 1984), thus obtaining  $e \lesssim 0.2$  (90% confidence level) and  $\chi^2_{\text{red}} \sim 1.4$ .

Using the estimated pulse period we folded the MECS lightcurves in the energy bands 1–3 keV, 3–6 keV and 6–10 keV, and the PDS lightcurves in the energy bands 13–25 keV and 25–80 keV, excluding the first 50 ks of our observation. The main pulse of the modulation presents a peak around phase 0.6. A secondary peak is visible around phase 0.1, which appears to be more prominent at higher energies. The pulse fraction, defined as  $(I_{\text{max}} - I_{\text{min}})/I_{\text{max}}$ , with  $I_{\text{max}}$  and  $I_{\text{min}}$  the maximum and minimum count rate, are  $(43 \pm 7)\%$ ,  $(57 \pm 6)\%$ ,  $(62 \pm 8)\%$ ,  $(7 \pm 2)\%$ , and  $(36 \pm 3)\%$  in the 1–3 keV, 3–6 keV, 6–10 keV, 13–25 keV, and 25–80 keV energy band, respectively. The pulse fraction in the 13–25 keV and 25–80 keV energy bands is strongly reduced by the presence of GX 9+1 in the PDS FOV (note however that the pulse fraction between 25–80 keV is somewhat higher because GX 9+1 is weaker at these energies). In Figure 6 we show the folded lightcurves in the energy bands 1–3 keV, 3–6 keV, 6–10 keV and 25–80 keV.

#### 4. Discussion

We have discovered a serendipitous source, SAX J1802.7–2017, in a BeppoSAX/NFI observation of the bright atoll source GX 9+1. SAX J1802.7–2017 shows coherent pulsations at a period of 139.612 s, indicating that the compact object in this system is most likely

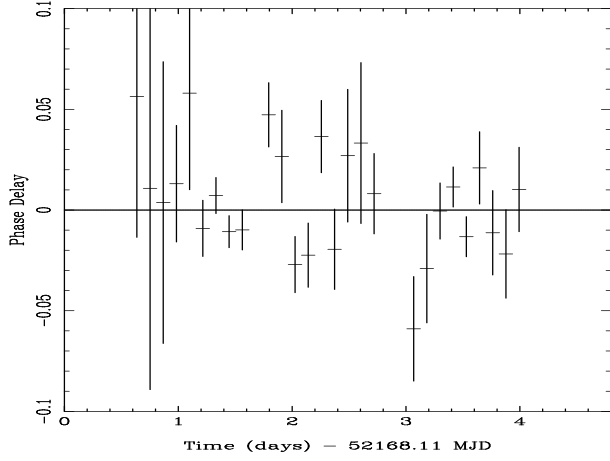


Fig. 5.— Phase delays after the barycentric correction with respect to the center of mass of the binary system.

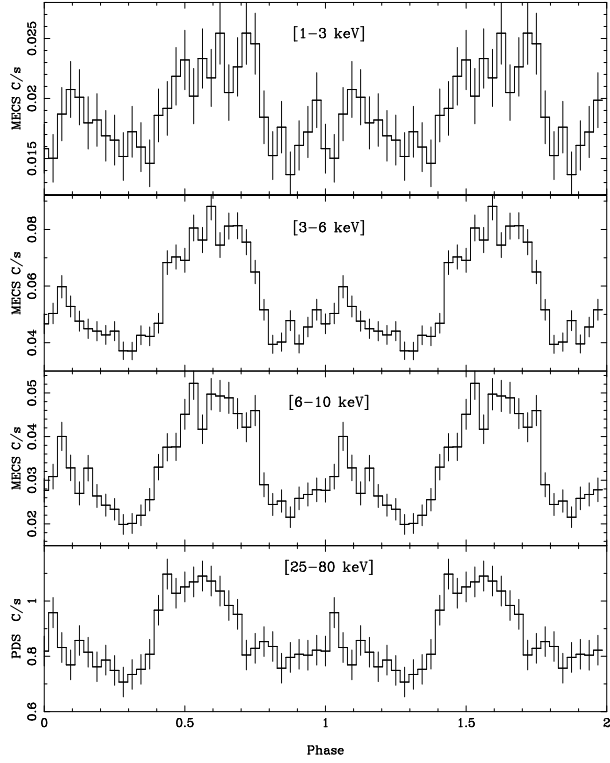


Fig. 6.— Folded lightcurves in four different energy bands. From the top to the bottom: 1–3 keV, 3–6 keV, 6–10 keV (MECS), 25–80 keV (PDS). The folding is obtained for a pulse period of 139.612 s and the zero epoch was assumed at the superior conjunction  $T_{\pi/2} = 52168.22$  MJD.

an accreting magnetic NS. Pulse arrival times show a sinusoidal modulation at a period of 4.6 days, which we interpret as due to the orbital motion of the source. The values of the orbital period and of the pulse period, as well as the pulse fraction in the MECS energy range ( $\sim 40\% - 60\%$ ), are consistent with the values usually found for HMXB systems (e.g. Oosterbroek et al. 1999; Bildsten et al. 1997).

The mass function of the system is

$$f(M) = \frac{M_C \sin^3 i}{(1+q)^2} = \left( \frac{2\pi}{P_{orb}} \right)^2 \frac{(a_x \sin i)^3}{G} \sim 17 \pm 5 M_{\odot},$$

where  $M_C$  is the companion star mass,  $G$  is the gravitational constant and  $q$  is the ratio of the compact object mass to the companion mass. The value of the mass function is not compatible with the system being a cataclysmic variable in which a white dwarf is orbiting a  $\sim 1 M_{\odot}$  companion. For a NS mass of  $1.4 M_{\odot}$  we have estimated a lower limit on the companion star mass,  $M_C \gtrsim 11 M_{\odot}$  (90% confidence level), typical of a HMXB. The epoch of the NS superior conjunction (which would correspond to the mid-eclipse time) derived from the fit of the orbital parameters falls during the first 50 ks of our observation, when the count rate of SAX J1802.7–2017 is compatible with the background count rate. This is compatible with the possible presence of an eclipse during the first 50 ks. Assuming that the eclipse ends  $\sim 0.58$  days after the beginning of our observation (52168.69 MJD, see Fig. 2) and taking into account that the zero epoch is  $0.11 \pm 0.10$  days, the half duration of the eclipse should be  $0.47 \pm 0.10$  days. The half-angle of the eclipse subtending the portion of circular orbit covered by the source is  $\theta = 0.64 \pm 0.14$  rad. The eclipse duration is related to the inclination angle  $i$  of the system by:  $R_C/a = (\cos^2 i + \sin^2 i \sin^2 \theta)^{1/2}$ , where  $R_C$  is the radius of a spherical primary star and  $a$  is (approximately) the separation between the two stars (see Primini et al. 1976). Then a rough lower limit on the companion star radius is  $R_C \gtrsim 14 R_{\odot}$ .

To estimate the luminosity of the source we performed a spectral analysis in the MECS range using the correct effective area for the position of the source in the MECS FOV (G. Cusumano, private communication). Although the low statistics of the data did not allow an accurate spectral analysis, we inferred a luminosity of  $\sim 5.6 \times 10^{35}$  erg/s over the 1.8–10 keV range by fitting the data to a power law (photon index  $-0.1 \pm 0.1$  and  $N_H = 1.7^{+0.8}_{-0.9} \times 10^{22}$  cm $^{-2}$ ) and assuming a source distance of 10 kpc. The lightcurve of the system shows a large variability suggesting that the system could be accreting via a stellar wind. This is also suggested by its long pulse period and relatively short orbital period, typical of HMXBs accreting via stellar wind such as Vela X-1 and 4U 1538–52 (see e.g. Corbet 1986; Nagase 1989). Indeed SAX J1802.7–2017 shows similarities to 4U 1538–52, which has a long spin period of  $\sim 529$  s, a short orbital period of  $\sim 3.7$  days, and a mass of  $19.8 \pm 3.3 M_{\odot}$ .

for the companion star (Reynolds, Bell, & Hilditch 1992). However, while the averaged luminosity of 4U 1538–52 and Vela X–1 is around  $5 \times 10^{36}$  ergs s $^{-1}$ , the averaged luminosity of SAX J1802.7–2017 measured during our observation is at least one order of magnitude lower (assuming an upper limit to the distance of 10 kpc). The source seems therefore to be quite underluminous with respect to massive binaries accreting via stellar wind, although more observations are needed to confirm this conclusion.

Note that, as the source has not been reported by other X-ray astronomy satellites before (in particular we did not find any detected source at the position of SAX J1802.7–2017 in ROSAT images, although the field of GX 9+1 was not observed by ASCA) it might well be a transient HMXB. Most of the transient HMXBs are Be-star systems (Liu et al. 2000). However, if SAX J1802.7–2017 belongs to this class it should be atypical considering that its orbital period and pulse period do not follow the Corbet correlation (Corbet 1986). Note also that the presence of an eccentricity cannot be excluded by our data, and more observations are needed to confirm the orbital parameters of the source.

We thank Dr. Giancarlo Cusumano for providing us the corrected effective area for our source and the anonymous referee for useful suggestions. This work was partially supported by the Italian Space Agency (ASI), by the Ministero della Istruzione, della Università e della Ricerca (MIUR) and the Netherlands Organization for Scientific Research (NWO).

## REFERENCES

Bildsten, L., Chakrabarty, D., Chiu, J., Finger, M. H., Koh,D. T., Nelson, R. W., et al. 1997, ApJS, 113, 367

Boella, G., Butler, R. C., Perola, G. C., et al. 1997a, A&AS, 122, 299

Corbet, R.H.D. 1986, MNRAS, 220, 1047

Frontera, F., Costa, E., dal Fiume, D., et al. 1997, A&AS, 122, 357

Leahy, D. A., Darbro, W., Elsner, R. F., et al. 1983, ApJ, 266, 160

Liu, Q. Z., van Paradijs, J., van den Heuvel, E.P.J. 2000, A&AS, 147, 25

Manzo, G., Giarrusso, S., Santangelo, A., et al. 1997, A&AS, 122, 341

Nagase, F. 1989, PASJ, 41, 1

Oosterbroek, T., Orlandini, M., Parmar, A. N., et al. 1999, A&AS, 351, L33

Parmar, A. N., Martin, D. D. E., Baudaz, M., et al. 1997, A&AS, 122, 309

Pereira, M.G., Braga, J., Jablonski, F., et al. 1999, ApJL, 526, L105

Primini, F., Rappaport, S., Joss, P. C., et al. 1976, ApJ, 210, L71

Reynolds, A. P., Bell, S. A., & Hilditch, R. W. 1992, MNRAS, 256, 631

Stella, L., White, N. E., & Rosner, R. 1986, ApJ, 308, 669

van der Klis, M., & Bonnet-Bidaud, J. M. 1984, A&A, 135, 155